Published in final edited form as:
Neurotoxicology. 2009 September ; 30(5): 794–802. doi:10.1016/j.neuro.2009.04.006.

Methylmercury disruption of embryonic neural development in Drosophila

Matthew D. Rand*, **Julie C. Dao**, and **Todd A. Clason**
Department of Anatomy and Neurobiology, College of Medicine, University of Vermont. College of Medicine, University of Vermont

Abstract

Methylmercury (MeHg) is a potent environmental neurotoxin that preferentially targets the developing embryonic nervous system. While a number of cytotoxic mechanisms of MeHg have been characterized in differentiated cells its mode of action in the developing nervous system *in vivo* is less clear. Studies in primate and rodent models demonstrate aberrant cell migration and disorganized patterning of cortical layers in the brain following MeHg exposure. However, defining the molecular and cellular pathways targeted by MeHg will require more genetically accessible animal models. In this study, we instigate a method of *in vitro* MeHg exposure using *Drosophila* embryos. We demonstrate dose-dependent inhibition of embryonic development with MeHg revealed by a failure of embryos to hatch to the larval stage. In addition, we document definitive phenotypes in neural development showing abnormalities in neuronal and glial cell patterning consistent with disrupted migration. As well, we observe pronounced defects in neurite outgrowth in both central and peripheral neurons. Ectopic expression of the Nrf2 transcription factor in embryos, a core factor in the antioxidant response element (ARE) pathway, enhances embryonic development and hatching in the presence of MeHg, illustrating the power of this model for investigation of candidate MeHg tolerance genes. Our data establish a utility for the *Drosophila* embryo model as a platform for elucidating MeHg sensitive pathways in neural development.

Introduction

Methylmercury (MeHg) is a potent environmental neurotoxin that persists in several species of fish common in the human diet. MeHg preferentially disrupts the developing nervous system, both pre- and postnatally. This toxicity has prompted stringent advisories for fish consumption for pregnant women, young children, and women of childbearing age. As a result, the risks of MeHg exposure versus the nutritional benefits of fish consumption have become a hotly debated topic (Myers *et al.* 2007; Oken and Bellinger 2008). It follows that understanding the mechanism by which MeHg induces abnormal development of embryonic neural tissues is of high priority, and yet it remains poorly understood.

The high affinity of MeHg for cellular thiol groups, on proteins and small molecule antioxidants such as glutathione (GSH), predicts that a vast number of targets exist in the cell. MeHg has been reported to disrupt a number of cellular functions via generating reactive oxygen species (Sarafian 1999); inhibiting protein synthesis, microtubule assembly and the cell cycle (Cheung

*to whom correspondence should be addressed: 149 Beaumont Ave, HSRF 426C, Burlington, VT 05405, (mdrand@zoo.uvm.edu), (802) 656-0405(Tel), (802) 656-4674(Fx).

and Verity 1985; Miura *et al.* 2000; Ponce *et al.* 1994); perturbing ion homeostasis (Sirois and Atchison 2000); and inducing apoptosis (Wilke *et al.* 2003). Most of these activities have been characterized in differentiated cells or tissues. Mechanisms of MeHg toxicity that are specific to developing neural tissues *in vivo* are less clear. Aberrant cell migration and disorganized patterning of cortical layers in prenatally exposed human brains (Choi *et al.* 1978) were observed in cases from the catastrophic MeHg exposures that occurred in Iraq in the 1970's. Similar outcomes are seen in primate and rodent models (Choi *et al.* 1978; Kakita *et al.* 2002; Peckham and Choi 1988), highlighting cell migration as a prominent target for disruption by MeHg. It is of note that cell death has not been a hallmark of prenatal MeHg exposure in humans (Choi *et al.* 1978). Thus, the neuropathology of early exposed nervous systems is consistent with the notion that MeHg can redirect the program of normal neural development, potentially through altering cell-cell signaling events that affect patterning and migration of neural tissues.

Evidence for MeHg affecting signaling pathways comes from in vitro studies, for example, in embryonic carcinoma cells where MeHg induces changes in expression levels of Eph and Ephrin, a receptor-ligand signaling pair that is important for axonal guidance (Wilson *et al.* 2005). MeHg can also alter neurotrophin signaling through the TrkA receptor in the neuronal PC12 cell line (Parran *et al.* 2004). *In vivo*, MeHg effects TrkA signaling in developing rat brains which parallels disruption of cortical lamina (Barone *et al.* 1998). We previously demonstrated that MeHg can alter signaling in the Notch receptor pathway (Bland and Rand 2006; Rand *et al.* 2008), a fundamental pathway for genesis and patterning of embryonic neural tissue. Aside from these examples, our understanding of the signaling pathways targeted by MeHg during neural development is incomplete. Furthermore, associating molecular targets of MeHg with developmental outcomes is inherently complex and could benefit from analyses in a simple genetic model organism.

In this study we instigate a model for *in vitro* MeHg exposure in Drosophila embryos. We demonstrate dose-dependent inhibition of embryonic development with MeHg as scored by a failure of embryos to hatch to the larval stage. In addition, we document characteristic phenotypes in neural development including abnormalities in neuron and glial cell patterning indicative of disrupted cell migration. As well, we observe defects in neurite outgrowth in both central and peripheral neurons. Ectopic expression of the Nrf2 transcription factor in embryos, which invokes the MeHg-protective antioxidant response element (ARE) pathway, enhances embryonic development in the presence of MeHg, illustrating the power of this model for investigation of putative MeHg tolerance genes. Altogether, these data establish the utility of a *Drosophila* embryo model as a platform for elucidating MeHg-sensitive pathways in neural development.

Methods

Fly lines and culture

Drosophila lines used include the Canton S; {ElavGal4, UAS-CD8-GFP, FLP} (Bloomington Drosophila Stock Center, #5146); gstD1-lacZ and UAS-Nrf2(UAS-CncC, Sykiotis and Bohmann 2008, gift from Dirk Bohmann); heat shock Gal4 (Bloomington Drosophila Stock Center). Flies were maintained at 25°C on standard cornmeal, molasses and agar medium with yeast. Standard crosses were performed between virgin female Gal4 driver lines and male UAS responder lines to generate F1 progeny to be tested.

MeHg treatments

Embryos were collected from a mating population in cages with grape agar plates seeded with yeast paste at 25°C. Embryos collected in a 2–5 hour laying period were allowed to develop

an additional 2 hours to reach the blastoderm cellularization stage (Stage 5). Embryos were then transferred to a nitex basket fabricated from the cap and top portion of a 50mL conical culture tube. Embryos were washed with tap water, dechorionated for 2 minutes in 50% bleach, and gently washed once gently in embryo wash (0.9 % NaCl, 0.1% Triton-X 100), followed by numerous washes by immersion in room temperature H_20. Embryos were dispersed in a monolayer on the nitex in the basket. Treatments were carried out by immersion of the basket in a reservoir of Robb's PBS (Robb 1969) containing MeHg or dimethylsulfoxide (DMSO) (0.1%) as a control. Methylmercury chloride (Aldrich, #442534) was prepared as a 50mM stock solution in DMSO. The final concentration of DMSO was 0.1% in all MeHg treatments. Reservoir levels were adjusted to allow the treatment solution to surround the embryos, leaving the top surface of the embryos exposed to air to optimize oxygen delivery and embryo development. Incubations were done at 18°C for 16–24 hours (equivalent to 8–12 hours development at 25°C).

Hatching and phenotype penetrance assays

Hatching from embryos to larvae was assayed by direct observation of embryos in nitex baskets in treatment reservoirs after 48 hours of development at 18°C. Hatching was determined by counting the number of empty vitelline membranes (hatched embryos) and unhatched embryos. Percent hatching was expressed as the [hatched/(hatched+unhatched)]×100. For treatments of the Canton S strain MeHg treatments were considered categorically with respect to control (0 MeHg) and statistical significance determined by a chi-square method.

Neural phenotypes were determined by abnormal cellular positioning (Elav stain in the case of PNS neurons and Eve stain in the case of CNS neurons) and neurite outgrowth defects (for 22C10 in the PNS and BP102 in the CNS). Preparations of stained embryos were mounted and observed in a blind fashion with respect to their treatment. For Elav staining, phenotypes were scored on the basis of a readily discernable defect in neural cell positioning in stage 13–16 embryos. For the PNS, a MeHg-induced trait was scored as "present" if abnormal positioning of Elav-stained neuron cell bodies within the dorsal, intermediate or ventral cluster of peripheral neurons was observed in at least one of the first three abdominal segments. For CNS axon phenotypes the BP102 staining pattern was used. An abnormal CNS axon phenotype was determined as a discernable thinning of longitudinal or commissural axon bundles in one or more of the first three abdominal segments. Phenotype frequency was determined as the percent of "present" phenotypes among the total embryos. The data is presented as the mean and standard deviation.

Live in vivo imaging

Embryos of the ElavGal4, UAS-CD8-GFP, FLP (EG4>GFP) line were prepared as above and incubated in nitex baskets on control or 20–50μM MeHg medium. Embryos were incubated at 18°C to the desired stage. Time-lapse imaging was performed with a Nikon SMZ1500 stereo dissecting microscope equipped with epiflourescence and a Spot Digital camera. Images were acquired with the Spot Insight software at 15-minute intervals over a period of 5 hours. Frames were processed into a movie sequence using ImageJ software (http://rsweb.nih.gov)

Immunostaining

Treated embryos were fixed in 500μL of a 50:50 mix of 8% paraformaldehyde in 0.1M PIPES, 2mM EGTA, 1mM $MgSO_4$, pH6.9 (PEM) with heptane by rocking for 25 minutes. Vitelline membranes were subsequently removed by removing the lower PEM layer and adding 750μL MeOH, then vortexing for 30 seconds. Settled embryos were collected, washed and stored at −20°C in methanol until staining. For immunostaining, embryos were permeablized in phosphate buffered saline (PBS) with 1% BSA, 0.1% triton X-100 (PBT). Subsequent blocking, primary and secondary antibody incubations were done in PBT with 5% each of

donkey and goat serum. Primary antibodies used were: mouse monoclonal anitbodies 22C10, BP102, anti-engrailed (4D9), anti-elav (9F8A9), anti-Repo (8D12) (Developmental Studies Hybridoma Bank, University of Iowa); anti-Evenskipped (3C10) (Chris Doe lab, University of Oregon); mouse anti-βgalactosidase (Sigma). Secondary antibodies used were: horseradish peroxidase (HRP)-conjugated anti-mouse (Jackson Immunoresearch) for diaminobenzidine substrate detection (DAB, ABC kit, Vectastain) using a standard protocol. Embryos were visualized by differential interference contrast (DIC, Nomarski optics) on a Leitz Orthoplan 2 microscope equipped with a Spot One digital camera and associated acquisition software (MVI, Avon MA). Images were assembled in Adobe Photoshop and Microsoft Powerpoint.

Nrf2 expression and rescue of hatching

Expression of Nrf2 was achieved using the Gal4>UAS combination with heat shockGal4 (hsG4) female flies mated to male UAS-Nrf2 (Nrf2) flies. Expression of Nrf2 was induced in 4-hour-old embryos by incubation at 37°C for 30 minutes and recovery at 25°C for various times. Embryos of control crosses (e.g. 1118>Nrf2; hsG4>1118) were treated with the same heat pulse protocol. Levels of Nrf2 mRNA expression were determined by real-time, quantitative polymerase chain reaction (qPCR) analysis using SYBR® Green dye (Sigma, Cat. No S5193) and an ABI PRISM 7500 Fast Sequence Detection System. Expression of target genes was normalized to expression of the RP49 ribosomal gene as a housekeeping gene as described previously (Rand *et al.* 2008). Primers for Nrf2 used were 5′-CATCAATGCCTCCTATGCCAG (sense) and 5′-CTTGTTGAAGCTCCTCCAGAG (antisense). Expression values were determined using the comparative $\Delta\Delta C_T$ method (Livak and Schmittgen 2001). Levels of Nrf2 expression in the hsG4>Nrf2 combination were compared to each of the parent strains (hsG4 and UAS-Nrf2) under identical heat pulse protocol and normalized to the Nrf2 level in the hsG4 line.

Percent hatching of embryos of control crosses (e.g. hsG4>1118, 1118>Nrf2) and Nrf2 over-expressing embryos (hsGal4>Nrf2) were determined with control (0 μM) and 20μM MeHg treatments. All embryos were exposed to the same heat pulse regimen as described for Nrf2 expression analysis above to induce gene expression. Hatching assays were performed as described above. Values are expressed as the percent hatching in MeHg relative to hatching in control treatment. The mean of three replicate determinations, with standard deviation, are presented. The difference of the mean hatching rates were compared by Student's *t*-test.

Results

Dose dependent MeHg inhibition of embryo development

We first established a method of reliable and accurate dosing of embryos with MeHg. Previously, we reported that dosage of 5–20μM MeHg in the food source of female flies resulted in developmental defects in embryos as determined by a decrease in hatching rate and neural phenotypes revealed by immunostaining (Rand *et al.* 2008). Furthermore, a dosage of 20μM MeHg in the food resulted in an approximate 3-fold increase in concentration of MeHg in embryos, which corresponded with a 50% decrease in subsequent hatching to larvae (Rand *et al.* 2008). However, this method often resulted in erratic cycles of egg (embryo) laying, which made reproducible staging and dosing of embryos difficult and impractical for high throughput experimentation. We therefore devised an *in vitro* method of introducing MeHg to embryos. This method permits collection of embryos laid within a narrow period of time prior to MeHg exposure, allowing for synchronized developmental staging. In addition, we found that aging embryos to approximately 3hrs, to the blastoderm stage (stage5–6), prior to MeHg exposure allows cellularization to occur and gives a more uniform effects of MeHg treatment on development. Incubation at 18°C was found to optimize embryo development and hatching in our system. Introduction of substances to Drosophila embryos has been notoriously difficult

primarily due to the lack of permeability of the waxy vitelline membrane (Margaritis *et al.* 1980). For example, embryo dechorionation, which requires immersion in 3% sodium hypochlorite (50% bleach), typically yields 80–90% viability due to exclusion of hypochlorite by the vitelline membrane. In contrast, MeHg showed an unusual ability permeate the dechorionated embryos, albeit with prolonged incubation. We presume this uptake is facilitated by inclusion of 0.1% DMSO in Robb's PBS incubation solution (see methods). MeHg exposure to the embryo was reflected in a decrease in the rate of hatching (Fig. 1). In separate analyses, we found that the carrier solvent, DMSO, at levels up to 10% showed no effect on hatching rate in this assay system (data not shown). Embryos showed a MeHg-concentration dependent decrease in hatching rate, with nearly 100% inhibition seen at 50μM MeHg (Fig. 1). Control treatments (0.1% DMSO alone) yielded ~80% hatching, with mild lethality likely stemming from manipulations of embryos during dechorionation and transfer steps. Significant decreases in hatching were seen at 10μM and 20μM MeHg treatments with more than 42% and 77% inhibition of hatching, respectively, relative to DMSO control (Fig. 1). These data confirm that MeHg is able to penetrate the vitelline membrane and adversely affect development of the embryo.

MeHg causes overall developmental delays but does not grossly perturb patterning of the embryonic tissues

Treatment of embryos with MeHg causes an overall delay in development. Developmental stage was determined by the position of the posterior tip of the ventral nerve cord (VNC) as revealed by the pan-neural antibody anti-HRP. The VNC arises from proliferating neuroblasts of the ventral neurectoderm. The VNC initially extends from the ventral medial surface around the posterior tip and along the dorsal region. Coincident with germ band retraction in the embryo, the VNC condenses to the ventral domain (Hartenstein 1993). In control treatments, embryos reached stage 14 in about 20 hours at 18°C (Fig. 2A, B). Treatments of 20–50μM MeHg caused a range of developmental delays. At 20μM MeHg, a majority of embryos develop to stage 14 with a delay of approximately 2–4 hours. In some instances, embryos showed more severe delays, including cessation of development at earlier stages and noticeable distortion of the tissues (Fig. 2E). In these instances, neurogenesis still occurred as determined by the presence of positively stained tissues with neural specific antibodies (Fig. 2E). The prevalence of developmentally delayed and distorted embryos was higher in 50μM MeHg exposures than at lower doses. The range of phenotypes observed likely results from subtle variations in stage among the embryos when they are exposed, as well as from variable permeability among individual embryos. Nonetheless, a significant number of embryos achieved stage 14 in each treatment such that comparative effects of equivalently staged embryos could be determined (e.g., compare Fig. 2A, B to C, D).

To further assess the overall effects of MeHg on developing embryonic tissues we evaluated the segmentation pattern of the embryo via expression of the Engrailed antigen. Engrailed is a transcription factor expressed in a stereotypical segmental array during stages 9–15 of embryonic development (Cui and Doe 1992). A banding pattern arises in the each of the thoracic and abdominal segments, which is readily detected with an antibody to the Engrailed protein. In stages 13–15 embryos, Engrailed expression is restricted to a row one to three cells wide of lateral ectodermal cells forming a dorsal-ventral stripe in the posterior edge of each segment (Fig. 3). Embryos exposed to 50μM MeHg that achieve stage 13–15 show no gross defect in the Engrailed pattern within the lateral ectodermal cells (Fig 3B). Engrailed staining also labels a stereotypical subset of neuroblasts and neurons in the VNC (Cui and Doe 1992). The segmentally reiterated arrangement of these CNS neurons is grossly similar between control and MeHg treatments (Fig. 3A and B). With 50μM MeHg, neurons within each segment in the VNC show subtle irregularity in positioning as compared to control (data not shown, also see Eve staining in Fig. 8). Together, these data indicate that the global patterning and

morphogenesis of the embryo is not perturbed with MeHg but suggests individual neurons are mislocalized within their segmental domains.

We next sought to determine if MeHg causes a non-specific disruption of tissue development in the embryo. Examination of embryos with Nomarski optics reveals the morphology of a number of ectodermally and endodermally derived structures, including the midgut and hindgut. The hindgut forms via involution of ectodermally derived cells that undergo proliferation during stages 8–10 (Hartenstein 1993). Involution of these cells forms a tubular structure with a defined sigmoidal "bend" in the dorsal region arising at stage 14–15. Stage 14–15 MeHg-treated embryos show no gross defect in formation of midgut and hindgut structures (Fig. 4B). In addition to the midgut, the bend in the hindgut is fortuitously labeled by the expression of a LacZ reporter for the gstD1 gene and shows a similar pattern between control and MeHg treatments (Fig. 4A and B). It is also of note that formation of the midgut, which requires fusion of inwardly migrating epithelial layers derived from anterior and posterior rudiments, is not appreciably disrupted by MeHg treatment.

MeHg-induced developmental delay is accompanied by defective nervous system formation

To assess the global effects of MeHg, we captured real-time images of nervous system development using a pan-neural GFP reporter construct. A combination consisting of the ElavGal4 driver and the UAS-CD8-GFP responder (EG4>GFP) results in expression of membrane localized GFP (by virtue of the CD8 fusion protein) in all neuroblasts and committed neurons. Timelapse imaging of EG4>GFP embryos reveals the appearance of neurons as they are born, the morphogenic movements that occur with condensation of the ventral nerve cord, and the birth and reiterated segmental patterning of peripheral neurons in the lateral domain (movie in Suppl. Data and Fig. 5A, B). In the presence of MeHg, VNC condensation is considerably delayed and completely stalls in some instances (movie in Suppl. Data and Fig. 5C). Formation of the PNS neurons occurs in an irregular pattern between neighboring segments as well (movie in Suppl. Data and Fig. 5C). While MeHg exposure was not seen to produce an abnormal overabundance of neural cells, gaps in the density of VNC neurons are occasionally seen (Fig. 5D), indicating aberrant positioning of neurons or possible inhibitory effects on neurogenesis causing a failure of neurons to be born.

Defects in PNS and CNS neural tissue patterning and axon outgrowth with MeHg exposure

For relevant comparisons of nervous system-specific effects between MeHg treatment and controls, the following analyses focused on embryos where development to stage 14–15 had successfully occurred as determined by condensation of the ventral nerve cord. The *Drosophila* peripheral nervous system (PNS) is comprised of sensory organs innervated by one or more neurons that develop in a stereotyped segmental pattern of clusters within the dorsal, lateral and ventral regions of the embryonic body wall ectoderm (Bodmer *et al.* 1989; Orgogozo and Grueber 2005). Staining for the Elav antigen, a neuron-specific nuclear-localized protein (Robinow and White 1991), reveals the relatively invariant, segmentally-repeated pattern of PNS neurons within the peripheral organs (Fig. 6A). Of note is the ordered, linear orientation of the five lch5 chordotonal organ neurons in the lateral cluster (Fig. 6A′) (see (Orgogozo and Grueber 2005)). With MeHg exposure, these neurons assume a disordered positioning, both with respect to the dorsal-ventral location of the cluster in the segment and among the adjacent neurons in the cluster (Fig. 6B, B′). No gross absence or excess of neurons was observed within PNS clusters with MeHg treatment, indicating that MeHg does not broadly inhibit or promote neurogenesis in the PNS.

With the clarity of this phenotype, we scored the penetrance of the disrupted neuronal patterning in a dose response to MeHg. Distorted PNS neuron positioning was seen at all

concentrations of MeHg with nearly 70% of embryos treated with 50μM MeHg exhibiting the phenotype (Fig. 6C).

PNS neuron morphology is revealed by staining with the 22C10/Futsch antibody that is specific for sensory neurons and labels dendrites, axons and the cell soma (Hummel *et al.* 2000). Control-treated embryos display a regular repeated array of neuronal architecture among the dorsal, lateral and ventral clusters of sensory organ neurons (Fig. 6D). Again, the linear adjacent orientation of the lch5 neurons in the lateral cluster is revealed by this antibody (Fig. 6D′). Axons projecting ventrally from the dorsal cluster, as well as from the lateral and ventral clusters, are seen to form complete projections to the VNC. Notable are the defined tracts of the segmental and intersegmental nerves along which project the lateral- and ventral-cluster axons (Fig. 6D′). MeHg treatment induces disruptions of the dorsal-ventral distribution of the PNS clusters among adjacent segments. In addition, axon and dendrite outgrowth is compromised with MeHg exposure (Fig 6E). Axons from the dorsal cluster projecting ventrally are stalled or follow a wavy path as compared to the straight projection of these axons in control embryos (Fig 6E, and data not shown). The intersegmental and segmental nerve tracts are incomplete or, where formed, show fusion to a single tract (Fig. 6E and data not shown). Overall, it is apparent that MeHg affects positioning and neurite outgrowth in developing PNS neurons.

Similar affects of MeHg on neuron positioning are seen in the central nervous system. Each hemisegment of the ventral neurectoderm is populated with 30 neuroblasts (NBs) that arise in stereotyped positions in each segment (Bossing *et al.* 1996). Neurons are subsequently born from asymmetric divisions of the NBs and their ganglion mother cell progeny. As a result, each neuron assumes a distinct position in the ventral nerve cord. NB and neuron position have been precisely mapped by virtue of expression of distinct antigenic epitopes, often residing on a transcription factor (Doe 1992). The Even-skipped (Eve) transcription factor is expressed in subsets of neurons in the ventral nerve cord, including the ventrally located EL, U and CQ neuron clusters and the dorsal aCC, pCC and RP2 motor neurons (Fujioka *et al.* 2003). These neurons assume a segmentally-repeated position within the cord that can be seen with anti-Eve staining of control embryos (Fig. 7A). As with the PNS, MeHg treatment causes disruption of the positional orientation of CNS neurons as revealed by eve staining. The most obvious phenotype is the uneven spacing of the dorsally located RP2 neurons that show abnormal positioning along the anterior-posterior axis (Fig. 7B″). The overall disorganized arrangement of the EL, U and CQ neurons with MeHg exposure is also revealed with Eve staining (Fig. 7B ′).

Axon projections within the VNC of CNS are also disrupted with MeHg as seen by staining with the BP102 antibody, which recognizes an antigen on all axons in the longitudinal and commissural tracts within the VNC (Fig. 8A). The mature CNS shows a normal “ladder-like” pattern of the parallel longitudinal tracts and connecting “rungs” of the anterior and posterior commissural connectives repeated within each segment (Fig. 8A). MeHg causes an incomplete formation of the longitudinal tract and a narrowing and sometime loss, of the longitudinal connectives. Similarly, thinning of the commissural bundles is seen with MeHg, indicating a diminished outgrowth of these CNS axons (Fig. 8B). We scored the penetrance of the CNS axon phenotype in a dose response to MeHg using the BP102 staining pattern. MeHg produces a concentration dependent increase in the occurrence of abnormally thin CNS axon bundles (Fig 8C). Interestingly, this phenotype showed to be less penetrant compared to PNS phenotypes (see Fig 6C), with less than 50% of embryos being affected at 50μM MeHg.

Glial patterning and migration are altered with MeHg

Drosophila glia are born from progenitors localized in the CNS (Sepp *et al.* 2000). Like their mammalian counterparts, *Drosophila* glia serve a supportive role for neurons by ensheathing

both the CNS and PNS axons. Unlike mammals, Drosophila produce far fewer glia than neurons, at approximately a 1:10 glia-neuron ratio (Hartenstein *et al.* 1998). Almost all glia arise from neural progenitors that also give rise to neurons. The pattern of glia in the CNS and PNS is revealed by staining for the Repo antigen, a glial-specific transcription factor (Xiong *et al.* 1994). Glia can be seen to decorate the longitudinal and commissural axon bundles of the ventral nerve cord as well as the tracts of the segmental and intersegmental nerves in the periphery of control stage 15 embryos (Fig. 9A). With MeHg exposure, glia show a distorted arrangement in the region of the longitudinal and commissural central axon bundles (Fig. 9B). Gaps in glia distribution are suggestive of abnormal migration of glia on underlying axons, or alternatively, an absence of the axonal structure at those sites. Many of the peripheral glia are born in the ventral neurectoderm and subsequently migrate to the periphery along the segmental and intersegmental nerve tracts (Sepp *et al.* 2000). We observe a concentration-dependent decrease in the number of glia in the periphery with MeHg exposure (Fig. 9C) suggesting that glia stall in their migration to the periphery. This is likely to correlate with incomplete formation of the segmental and intersegmental axon tracts seen above. Cell counts of glia per segment of the CNS showed that MeHg treatment does not significantly alter the number of glia produced relative to untreated controls (data not shown).

MeHg tolerance invoked by Nrf2 expression

The above phenotypes suggest the Drosophila embryo model will prove highly effective for evaluating genes that function in MeHg tolerance. Expression of transgenes in flies is easily achieved with the Gal4-UAS heterologous expression system (Brand *et al.* 1994). As a first approach, we have examined the ability of over-expression of the Nrf2 transcription factor, which acts upon the antioxidant response element (ARE), to confer MeHg tolerance. Activation of the ARE invokes upregulation of phase II antioxidant genes, which have the ability to protect against MeHg in cultured cells (Toyama *et al.* 2007). The genetic combination of heatshock-Gal4 and UAS-Nrf2 (hsG4>Nrf2) responded to a heat pulse with more than a 50-fold up-regulation of Nrf2 mRNA at 3 hours and 9-fold higher Nrf2 levels at 6 hours after induction relative to Nrf2 expression in embryos of similarly heat shocked parent fly lines (Fig 10A). The ability of Nrf2 expression to confer tolerance to MeHg was assayed by via embryo hatching in the presence versus absence of MeHg (Fig. 10B). The hsG4>Nrf2 embryos showed a significantly higher percentage of hatching (51.8%) on 20μM MeHg than the hsG4>1118 embryos (27.4%) or the 1118>Nrf2 embryos (13.0%) indicating that upregulated Nrf2 expression confers tolerance to MeHg. Together, these data demonstrate the effectiveness of the Drosophila embryo model in assaying activity of candidate MeHg tolerance genes.

Discussion

We demonstrate the profound effects of MeHg on disrupting embryonic nervous system development in the Drosophila model. Whereas overall development is delayed by MeHg exposure, defects in patterning, positioning and maturation of neurons and glia in the CNS and PNS are pronounced and suggestive of a preference of MeHg toward disrupting these tissues. We predict these neural-related phenotypes will prove to be powerful endpoints to investigate MeHg mechanisms in future assays. Toward this goal, we demonstrate that ectopic expression of the Nrf2 transcription factor is able confer tolerance to MeHg, illustrating the power of the Drosophila model for assaying specific gene candidates in the role of MeHg tolerance mechanisms. The implication of this model and these findings for understanding MeHg neurotoxic mechanisms and for development of future assays is discussed below.

MeHg elicits lethality and neural phenotypes in embryos in a somewhat parallel dose-dependent manner. Of note is the relatively high levels of MeHg (10–50μM range) required to induce phenotypes compared to lethal dosages typically found in cell culture models (0.1–

10μM range). In these treatments, we have not determined the amount of MeHg that successfully permeates the embryo. In this regard, the degree to which vitelline membrane of the fly embryo permits solute transport is not well known. It is possible that the considerably lower levels of MeHg exist in the embryo relative to MeHg in the ambient medium in these experiments. Determining the MeHg concentration that embryonic cells are exposed to poses a challenge since the vitelline membrane is highly proteinaceous and a likely reservoir for MeHg that will confound interpretation of mercury analyses of treated embryos. Alternatively, in the case where MeHg freely passes into the embryo, the elevated dose required for embryo phenotypes may reflect an overall higher tolerance of cells to MeHg when they are in the context of a tissue versus isolated in culture. In either case, it is apparent that this model, in its current stage of development, is not suitable for extrapolating relevant dose responses to mammalian cell or animal models. Nonetheless, this model affords the possibility to dissect cell type specific effects of MeHg in a pertinent developmental context.

MeHg disrupts patterns of neuron localization and neurite outgrowth with MeHg exposure, in both the CNS and PNS, which suggests a common mechanism affects these cells. Histopathological investigation of postmortem brains from cases of infant MeHg poisoning in Iraq implicated a role for aberrant cell migration (Choi *et al.* 1978). Indeed, MeHg potently inhibits cell migration in cultured neurons (Sass *et al.* 2001). Furthermore, the fact that MeHg disrupts microtuble polymerization (Vogel *et al.* 1985) is consistent with this mechanistic model. It is therefore likely that MeHg affects the cytoskeletal elements of neurons in the fly embryo, preventing them from successfully acquiring their appropriate position and debilitating neurite outgrowth. However, the specificity with which this mechanism acts upon neurons *in vivo* is poorly understood. It does not appear that microtubule function is targeted equally in all cell types in the *Drosophila* embryo since cells of the midgut and hindgut show proper migration and fusion events. A closer comparative examination of MeHg susceptibility of developing neurons and gut cells in this system will yield a better understanding of the cell type specificity of microtubule targets.

Alternatively, MeHg could act to debilitate cell-cell signaling that guides positioning of neurons and targeting of growing neurites. Consistent with this mechanism, it has been shown that MeHg alters expression of components of the Eph/Ephrin pathway, a conserved pathway that regulates neuronal migration and neurite pathfinding (Wilson *et al.* 2005). Interestingly, upregulation of certain Eph/Ephrin pathway members can result in stalled axon outgrowth in rat striatal neurons (Gao *et al.* 2000). Similar outcomes occur with manipulated expression of Eph/Ephrin orthologs in *Drosophila* (Bossing and Brand 2002). Our embryo model system therefore presents a powerful tool to investigate potential effect of MeHg that are mediated by Eph signaling, and other signaling pathways, that regulate neurite outgrowth and migration in the developing nervous system.

We observe that glial patterning, similar to neurons, is highly disordered with MeHg exposure. While MeHg has no gross effect on the number of glia propagated, their arrangement along the CNS scaffolding is irregular. *Drosophila* glia, which arise from a restricted number of glioblast precursors, typically undergo migration to assume their final position before ensheathing axon bundles (Hartenstein *et al.* 1998). Most notably, peripheral glia, which are born in the CNS, migrate long distances and ensheath the entirety of sensory neurons by the end of embryogenesis (Sepp *et al.* 2000). A decreased presence of glia in the periphery following MeHg exposure suggests that glial migration is strongly inhibited by MeHg. However, peripheral glia and sensory neurons are known to rely on reciprocal interactions for their development (Sepp and Auld 2003). Thus, this analysis cannot distinguish whether MeHg preferentially targets glia, neurons or both. Nonetheless, future analyses using of transgenic expression of MeHg-protective genes (e.g. Nrf2) specifically in glia versus neurons, will yield insight into this important unresolved question.

Clearance of MeHg from cells is mediated predominantly by complexation with glutathione (GSH) and subsequent export (Kerper *et al.* 1996). Accordingly, upregulation of GSH can render protection to MeHg toxicity (Kaur *et al.* 2006). The antioxidant response element (ARE) is a master regulator of genes that combat oxidative stress, including genes involved in GSH synthesis and redox status (Osburn and Kensler 2008). Modulation of the ARE by the Nrf2 transcription factor can afford protection to MeHg in mammalian cells (Toyama *et al.* 2007). Here we show the *Drosophila* homolog of Nrf2 can similarly afford protection to the developing embryo exposed to MeHg. MeHg can induce ARE activation through Nrf2 in rat astrocytes, suggesting that the ARE pathway could mediate an important defense to MeHg insult (Wang *et al.* 2008). A recent elaboration of the conserved nature of the Nrf2, and its regulator Keap1, and ARE signaling in *Drosophila* makes this model a powerful means to investigate the contribution of this pathway to MeHg protective mechanisms in vivo.

The identity of pathways targeted by MeHg in neural development are not well resolved. We have previously identified an activity for MeHg in activation of Notch target genes (Bland and Rand 2006; Rand *et al.* 2008). While embryonic exposure to MeHg can induce changes in Notch target gene transcripts, it is unclear whether MeHg-altered Notch signaling can impact developmental outcomes in embryonic tissues. Global activation of Notch signals by genetic means results in a failure of neurons to form due to altered cell fates in the neurectoderm (Artavanis-Tsakonas *et al.* 1991). We anticipate that MeHg-induced activation of Notch would cause a failure of neurons to form in the embryo. We do not observe a gross deficiency in numbers of neurons in the CNS or PNS of MeHg-treated embryos, suggesting that the level of Notch activation with MeHg is not sufficient to induce such a global phenotype. However, Notch signals act at several levels, for example, in the control of sibling neuron identity and in the outgrowth of neurites (Berezovska *et al.* 1999; Skeath and Doe 1998). It is possible that MeHg-induced Notch signaling could contribute to the failure of neurite outgrowth seen in the CNS and PNS. We anticipate that further experiments employing available fly strains harboring transgenes that modulate the Notch pathway will help pinpoint the action of MeHg upon Notch in a neural developmental context.

Distinguishing the action of MeHg upon structural versus signaling constituents of the cell during development remains a prominent focus of research in MeHg toxicity. Much has been learned from the application of MeHg to defined homogeneous cell culture models. However, advancing understanding of developmental consequences of MeHg toxicity requires analysis of developmental events in relevant tissues *in vivo*. We foresee that further development and application of the *Drosophila* embryo model described here will be an invaluable tool for investigation of fundamental candidate genes and pathways of MeHg neurotoxicity mechanisms.

Supplementary Material

Refer to Web version on PubMed Central for supplementary material.

Acknowledgments

We thank Dirk Bohmann (University of Rochester, NY) for the gstD1-LacZ and UAS-CncC flies, and Chris Doe (Univ. of Oregon) for Even-skipped antibody. Antibodies from the hybridoma lines for 22C10, BP102, FasII, Elav, Repo and Engrailed developed by a number of investigators, were obtained from the Developmental Studies Hybridoma Bank developed under the auspices of the NICHD and maintained by The University of Iowa, Department of Biological Sciences, Iowa City, IA 52242. (This work was supported by NIEHS ES015550 awarded to M.D.R)

References

Artavanis-Tsakonas S, Delidakis C, Fehon RG. The Notch locus and the cell biology of neuroblast segregation. Annu Rev Cell Biol 1991;7:427–52. [PubMed: 1809352]

Barone S Jr, Haykal-Coates N, Parran DK, Tilson HA. Gestational exposure to methylmercury alters the developmental pattern of trk-like immunoreactivity in the rat brain and results in cortical dysmorphology. Brain Res Dev Brain Res 1998;109:13–31.

Berezovska O, McLean P, Knowles R, Frosh M, Lu FM, Lux SE, Hyman BT. Notch1 inhibits neurite outgrowth in postmitotic primary neurons. Neuroscience 1999;93:433–9. [PubMed: 10465425]

Bland CE, Rand MR. Methylmercury induces activation of Notch signaling. Neurotoxicology 2006;27:982–91. [PubMed: 16757030]

Bodmer R, Carretto R, Jan YN. Neurogenesis of the peripheral nervous system in Drosophila embryos: DNA replication patterns and cell lineages. Neuron 1989;3:21–32. [PubMed: 2515889]

Bossing T, Brand AH. Dephrin, a transmembrane ephrin with a unique structure, prevents interneuronal axons from exiting the Drosophila embryonic CNS. Development 2002;129:4205–18. [PubMed: 12183373]

Bossing T, Udolph G, Doe CQ, Technau GM. The embryonic central nervous system lineages of Drosophila melanogaster. I. Neuroblast lineages derived from the ventral half of the neuroectoderm. Developmental biology 1996;179:41–64. [PubMed: 8873753]

Brand AH, Manoukian AS, Perrimon N. Ectopic expression in Drosophila. Methods in cell biology 1994;44:635–54. [PubMed: 7707973]

Cheung MK, Verity MA. Experimental methyl mercury neurotoxicity: locus of mercurial inhibition of brain protein synthesis in vivo and in vitro. Journal of neurochemistry 1985;44:1799–808. [PubMed: 3845956]

Choi BH, Lapham LW, Amin-Zaki L, Saleem T. Abnormal neuronal migration, deranged cerebral cortical organization, and diffuse white matter astrocytosis of human fetal brain: a major effect of methylmercury poisoning in utero. J Neuropathol Exp Neurol 1978;37:719–33. [PubMed: 739273]

Cui X, Doe CQ. ming is expressed in neuroblast sublineages and regulates gene expression in the Drosophila central nervous system. Development 1992;116:943–52. [PubMed: 1339340]

Doe CQ. Molecular markers for identified neuroblasts and ganglion mother cells in the Drosophila central nervous system. Development 1992;116:855–63. [PubMed: 1295739]

Fujioka M, Lear BC, Landgraf M, Yusibova GL, Zhou J, Riley KM, Patel NH, Jaynes JB. Even-skipped, acting as a repressor, regulates axonal projections in Drosophila. Development 2003;130:5385–400. [PubMed: 13129849]

Gao PP, Sun CH, Zhou XF, DiCicco-Bloom E, Zhou R. Ephrins stimulate or inhibit neurite outgrowth and survival as a function of neuronal cell type. Journal of neuroscience research 2000;60:427–36. [PubMed: 10797545]

Hartenstein, V. Atlas of Drosophila Development. Cold Spring Harbor Press; New York: 1993.

Hartenstein V, Nassif C, Lekven A. Embryonic development of the Drosophila brain. II. Pattern of glial cells. The Journal of comparative neurology 1998;402:32–47. [PubMed: 9831044]

Hummel T, Krukkert K, Roos J, Davis G, Klambt C. Drosophila Futsch/22C10 is a MAP1B-like protein required for dendritic and axonal development. Neuron 2000;26:357–70. [PubMed: 10839355]

Kakita A, Inenaga C, Sakamoto M, Takahashi H. Neuronal migration disturbance and consequent cytoarchitecture in the cerebral cortex following transplacental administration of methylmercury. Acta Neuropathol 2002;104:409–17. [PubMed: 12200629]

Kaur P, Aschner M, Syversen T. Glutathione modulation influences methyl mercury induced neurotoxicity in primary cell cultures of neurons and astrocytes. Neurotoxicology 2006;27:492–500. [PubMed: 16513172]

Kerper LE, Mokrzan EM, Clarkson TW, Ballatori N. Methylmercury efflux from brain capillary endothelial cells is modulated by intracellular glutathione but not ATP. Toxicology and applied pharmacology 1996;141:526–31. [PubMed: 8975777]

Livak KJ, Schmittgen TD. Analysis of relative gene expression data using real-time quantitative PCR and the 2(−Delta Delta C(T)) Method. Methods 2001;25:402–8. [PubMed: 11846609]

Margaritis LH, Kafatos FC, Petri WH. The eggshell of Drosophila melanogaster. I. Fine structure of the layers and regions of the wild-type eggshell. Journal of cell science 1980;43:1–35. [PubMed: 6774986]

Miura K, Himeno S, Koide N, Imura N. Effects of methylmercury and inorganic mercury on the growth of nerve fibers in cultured chick dorsal root ganglia. Tohoku J Exp Med 2000;192:195–210. [PubMed: 11249149]

Myers GJ, Davidson PW, Strain JJ. Nutrient and methyl mercury exposure from consuming fish. The Journal of nutrition 2007;137:2805–8. [PubMed: 18029503]

Oken E, Bellinger DC. Fish consumption, methylmercury and child neurodevelopment. Current opinion in pediatrics 2008;20:178–83. [PubMed: 18332715]

Orgogozo, V.; Grueber, WB. FlyPNS, a database of the Drosophila embryonic and larval peripheral nervous system; BMC developmental biology. 2005. p. 4www.normalesup.org/~vorgogoz/FlyPNS/page1.html

Osburn WO, Kensler TW. Nrf2 signaling: an adaptive response pathway for protection against environmental toxic insults. Mutation research 2008;659:31–9. [PubMed: 18164232]

Parran DK, Barone S Jr, Mundy WR. Methylmercury inhibits TrkA signaling through the ERK1/2 cascade after NGF stimulation of PC12 cells. Brain Res Dev Brain Res 2004;149:53–61.

Peckham NH, Choi BH. Abnormal neuronal distribution within the cerebral cortex after prenatal methylmercury intoxication. Acta Neuropathol (Berl) 1988;76:222–6. [PubMed: 3213424]

Ponce RA, Kavanagh TJ, Mottet NK, Whittaker SG, Faustman EM. Effects of methyl mercury on the cell cycle of primary rat CNS cells in vitro. Toxicology and applied pharmacology 1994;127:83–90. [PubMed: 8048057]

Rand MD, Bland CE, Bond J. Methylmercury activates enhancer-of-split and bearded complex genes independent of the notch receptor. Toxicol Sci 2008;104:163–76. [PubMed: 18367466]

Robb JA. Maintenance of imaginal discs of Drosophila melanogaster in chemically defined media. The Journal of cell biology 1969;41:876–85. [PubMed: 5768877]

Robinow S, White K. Characterization and spatial distribution of the ELAV protein during Drosophila melanogaster development. Journal of neurobiology 1991;22:443–61. [PubMed: 1716300]

Sarafian TA. Methylmercury-induced generation of free radicals: biological implications. Met Ions Biol Syst 1999;36:415–44. [PubMed: 10093932]

Sass JB, Haselow DT, Silbergeld EK. Methylmercury-induced decrement in neuronal migration may involve cytokine-dependent mechanisms: a novel method to assess neuronal movement in vitro. Toxicol Sci 2001;63:74–81. [PubMed: 11509746]

Sepp KJ, Auld VJ. Reciprocal interactions between neurons and glia are required for Drosophila peripheral nervous system development. J Neurosci 2003;23:8221–30. [PubMed: 12967983]

Sepp KJ, Schulte J, Auld VJ. Developmental dynamics of peripheral glia in Drosophila melanogaster. Glia 2000;30:122–33. [PubMed: 10719354]

Sirois JE, Atchison WD. Methylmercury affects multiple subtypes of calcium channels in rat cerebellar granule cells. Toxicology and applied pharmacology 2000;167:1–11. [PubMed: 10936073]

Skeath JB, Doe CQ. Sanpodo and Notch act in opposition to Numb to distinguish sibling neuron fates in the Drosophila CNS. Development 1998;125:1857–65. [PubMed: 9550718]

Sykiotis GP, Bohmann D. Keap1/Nrf2 signaling regulates oxidative stress tolerance and lifespan in Drosophila. Developmental cell 2008;14:76–85. [PubMed: 18194654]

Toyama T, Sumi D, Shinkai Y, Yasutake A, Taguchi K, Tong KI, Yamamoto M, Kumagai Y. Cytoprotective role of Nrf2/Keap1 system in methylmercury toxicity. Biochemical and biophysical research communications 2007;363:645–50. [PubMed: 17904103]

Vogel DG, Margolis RL, Mottet NK. The effects of methyl mercury binding to microtubules. Toxicology and applied pharmacology 1985;80:473–86. [PubMed: 4035699]

Wang L, Jiang H, Yin Z, Aschner M, Cai J. Methylmercury Toxicity and Nrf2-dependent Detoxification in Astrocytes. Toxicol Sci. 2008

Wilke RA, Kolbert CP, Rahimi RA, Windebank AJ. Methylmercury induces apoptosis in cultured rat dorsal root ganglion neurons. Neurotoxicology 2003;24:369–78. [PubMed: 12782102]

Wilson DT, Polunas MA, Zhou R, Halladay AK, Lowndes HE, Reuhl KR. Methylmercury alters Eph and ephrin expression during neuronal differentiation of P19 embryonal carcinoma cells. Neurotoxicology 2005;26:661–74. [PubMed: 15990172]

Xiong WC, Okano H, Patel NH, Blendy JA, Montell C. repo encodes a glial-specific homeo domain protein required in the Drosophila nervous system. Genes & development 1994;8:981–94. [PubMed: 7926782]

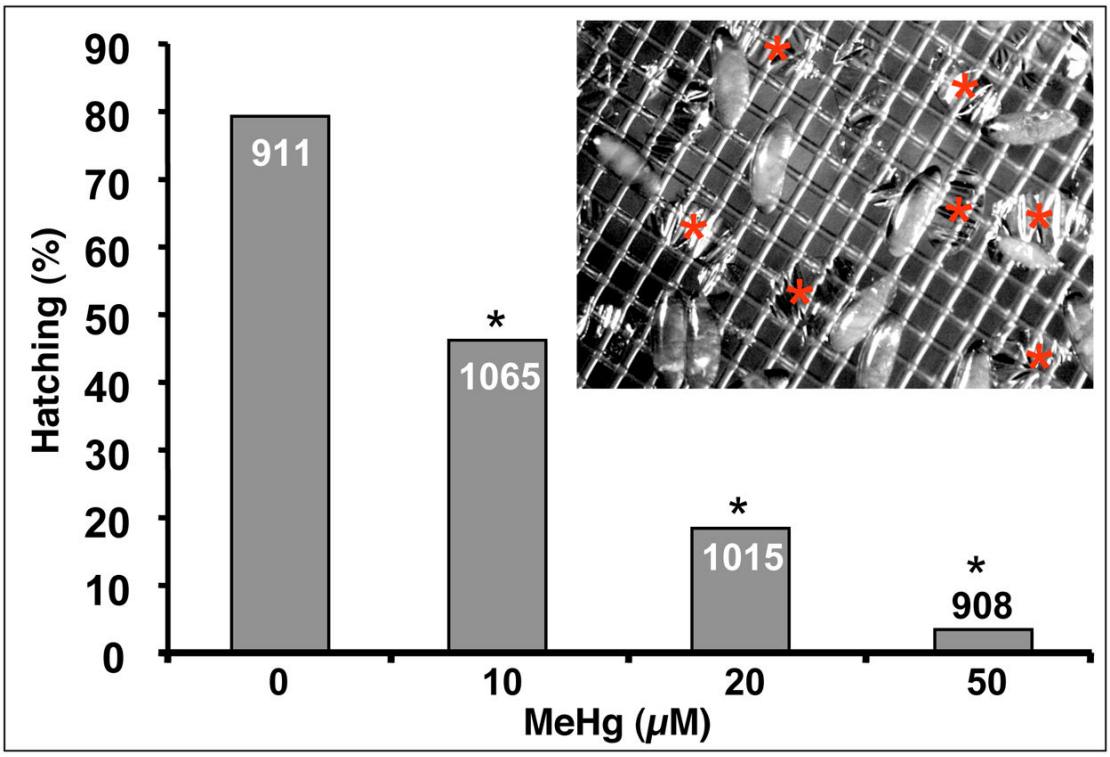

Figure 1. Methylmercury induced lethality in Drosophila embryos

Hatching of dechorionated embryos suspended in Robb's PBS with indicated concentration of MeHg was scored after 48 hours of development at 18°C. Inset shows an image of unhatched and hatched embryos suspended on nitex within the basket. The remaining empty vitelline membranes (red asterix) are scored as hatched embryos. Hatching rates for the sum of two independent series of MeHg treatments of embryos is shown. (* is $p<0.001$ by chi-square. For each treatment category n=number in bar)

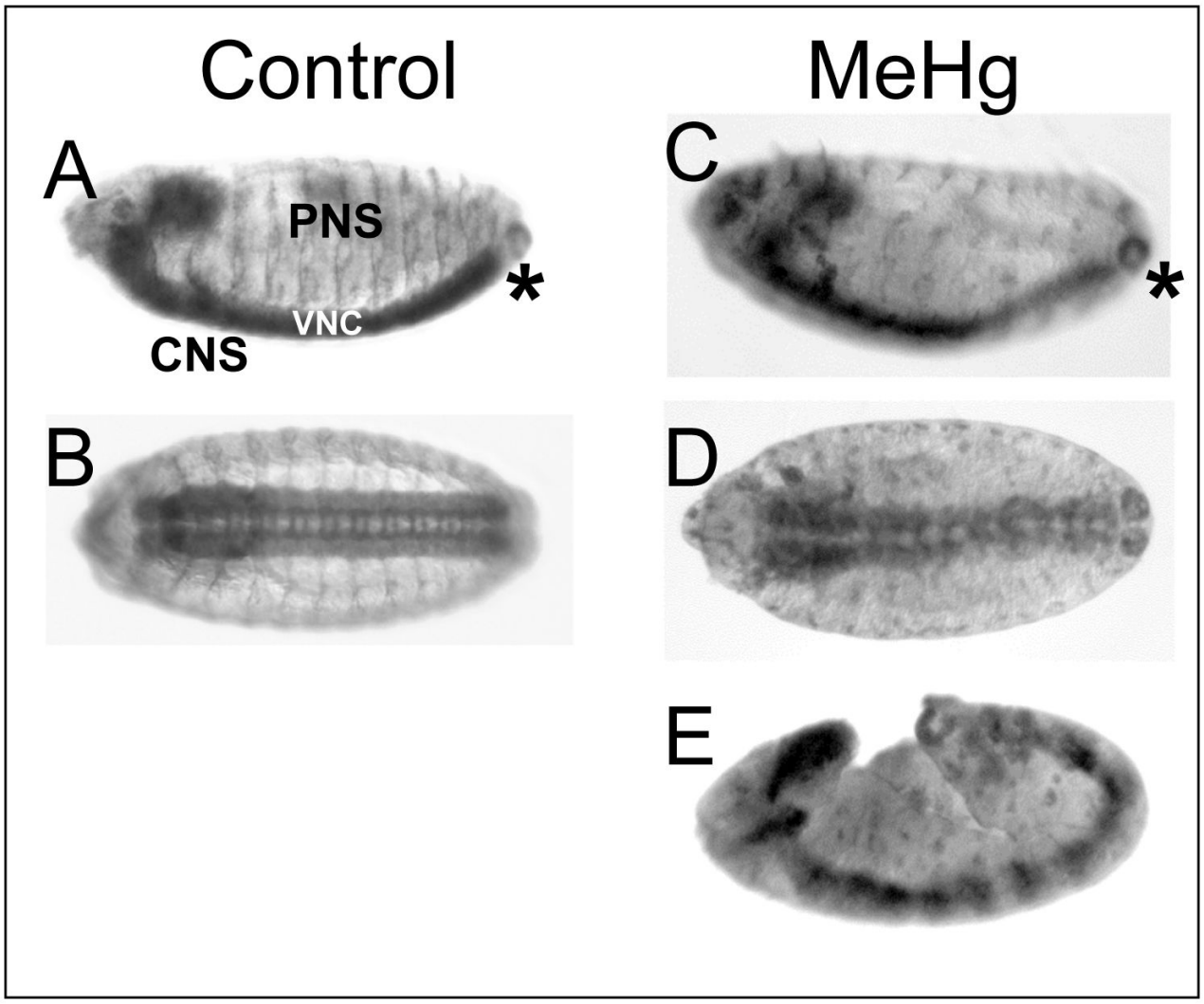

Figure 2. Effects of MeHg on embryonic development

Stage 14 embryos are identified by features of the central nervous system (CNS) and peripheral nervous system (PNS) revealed with the anti-HRP pan-neural specific antibody (anterior is to the left in all images, lateral orientation in A, C and E; ventral view in B and D). Similarly staged embryos are identified by the position of the posterior terminus (*) of the ventral nerve cord (VNC). Control embryos (A, B) show normal development of the CNS and PNS reaching stage 14 at 20 hours at 18°C. MeHg treatments delay development with stage 14 achieved in 22–24 hours (C, D). Gross defects in the CNS and PNS are evident with 20μM MeHg treatment (C, D). In some cases, severe developmental delay and stalling is seen with 50μM MeHg exposure (E).

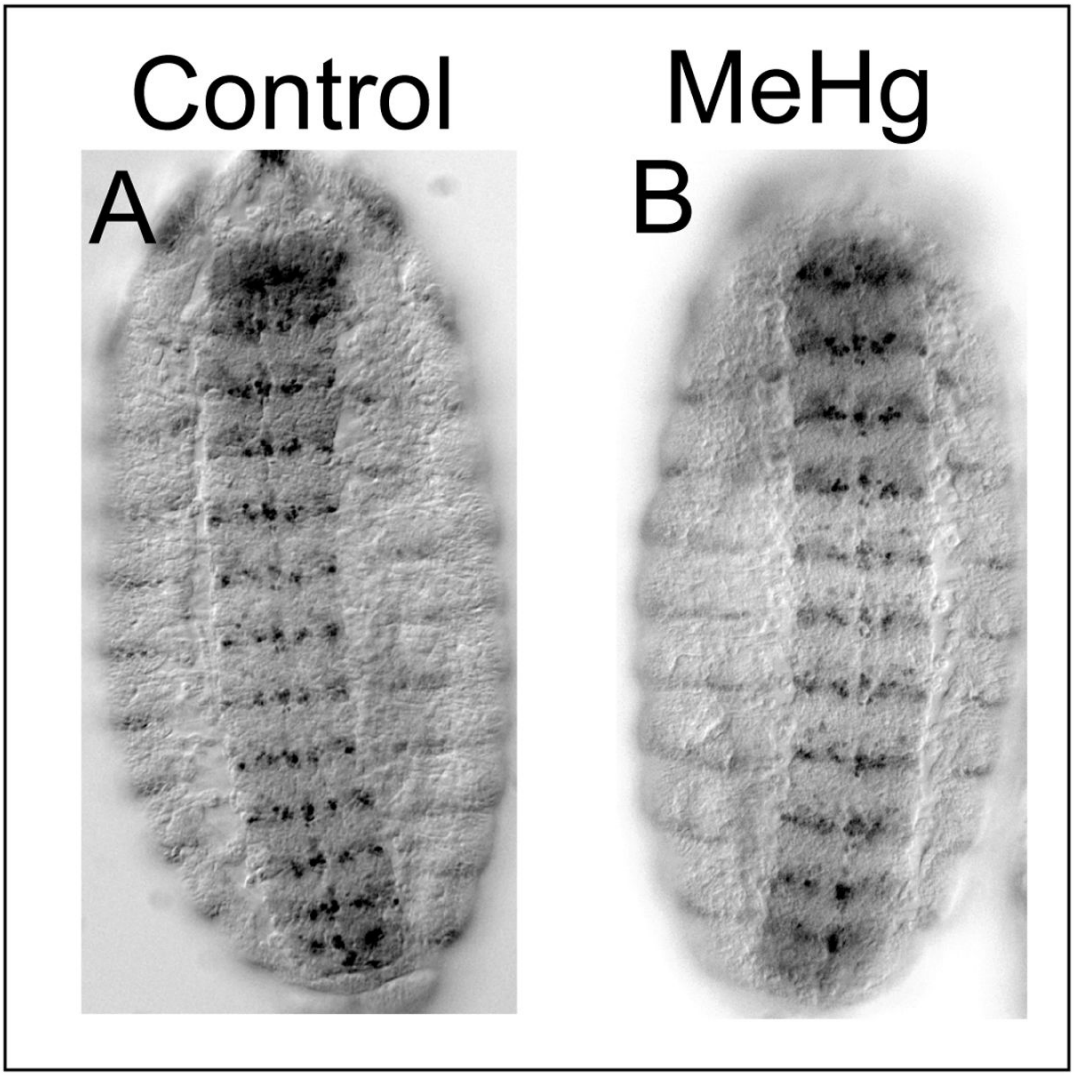

Figure 3. Segmental patterning in MeHg treated embryos

The Engrailed antibody stains a row of ectodermal cells in the lateral region as well a subsets of neuroblasts and neuron in the VNC. Overall segmental pattern of Engrailed expression is not disrupted in MeHg (50μM) treated embryos (B) compared to controls (A). Embryos are oriented in a ventral view with the anterior up.

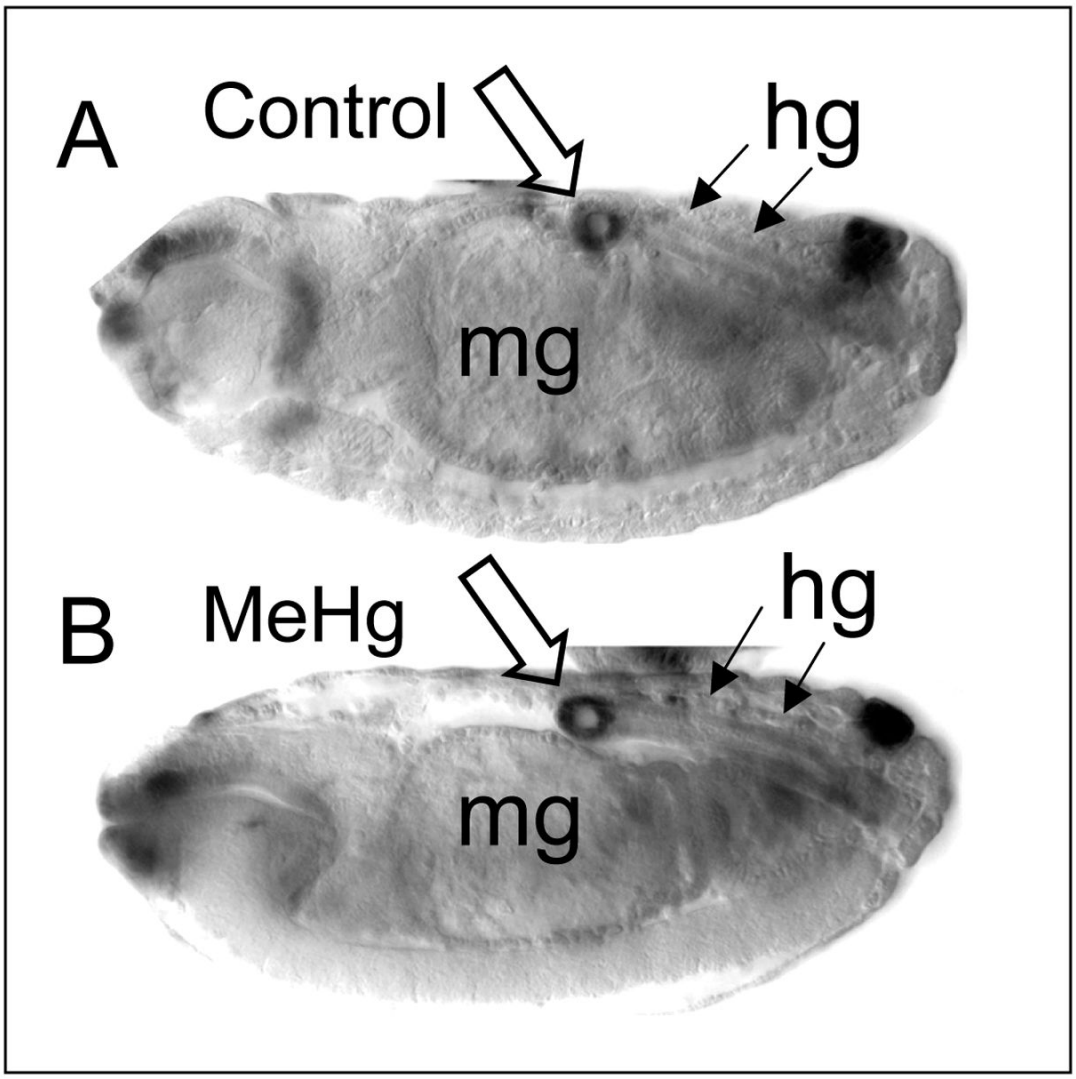

Figure 4. Development of non-neural tissues in MeHg treated embryos

Stage 14 embryos obtained after control (A) or 20μM MeHg (B) exposure during development. Embryos carry a lacZ reporter for the glutathione S-transferase D1 gene (gstD-lacZ), which is expressed in cells of the midgut (mg) and hindgut (hg). Elements of the midgut and hindgut, including the characteristic bend in the hindgut (open arrow, strongly labeled and seen in cross section in this Nomarski image), are properly formed in both control and MeHg treated embryos (anterior is to the left and dorsal is up).

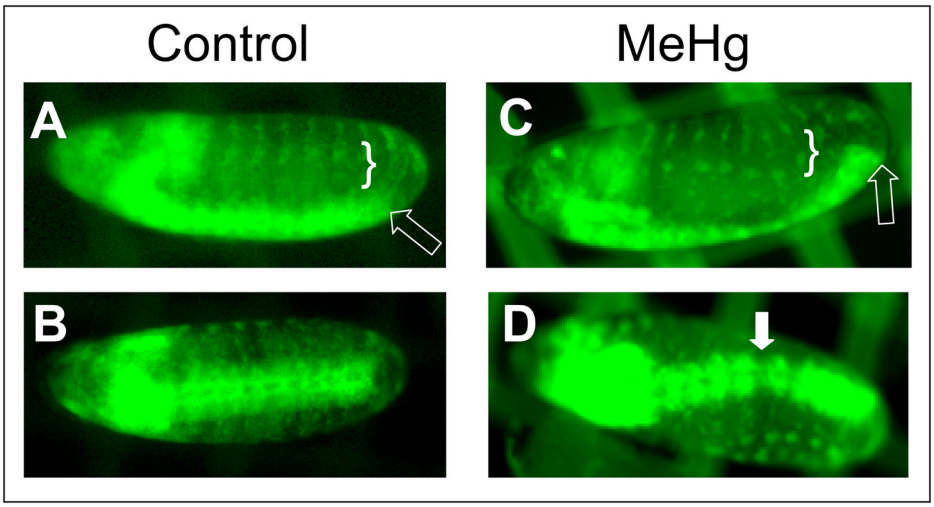

Figure 5. Disrupted neural development in MeHg treated embryos

The PNS and CNS of ElavGal4>UAS-CD8-GFP embryos are reveled under epiflourescence (anterior is to the left in all images, lateral orientation in A and C; ventral in B and D). Images of embryos used for timelapse imaging are shown control (A, B) and 20μM MeHg treated (C, D). Stage 14–15 embryos are shown as determined by VNC condensation (open arrows). Disrupted patterning in the PNS (bracket) and gaps in the CNS (filled arrow) are seen with MeHg exposure during development (also see supplemental data).

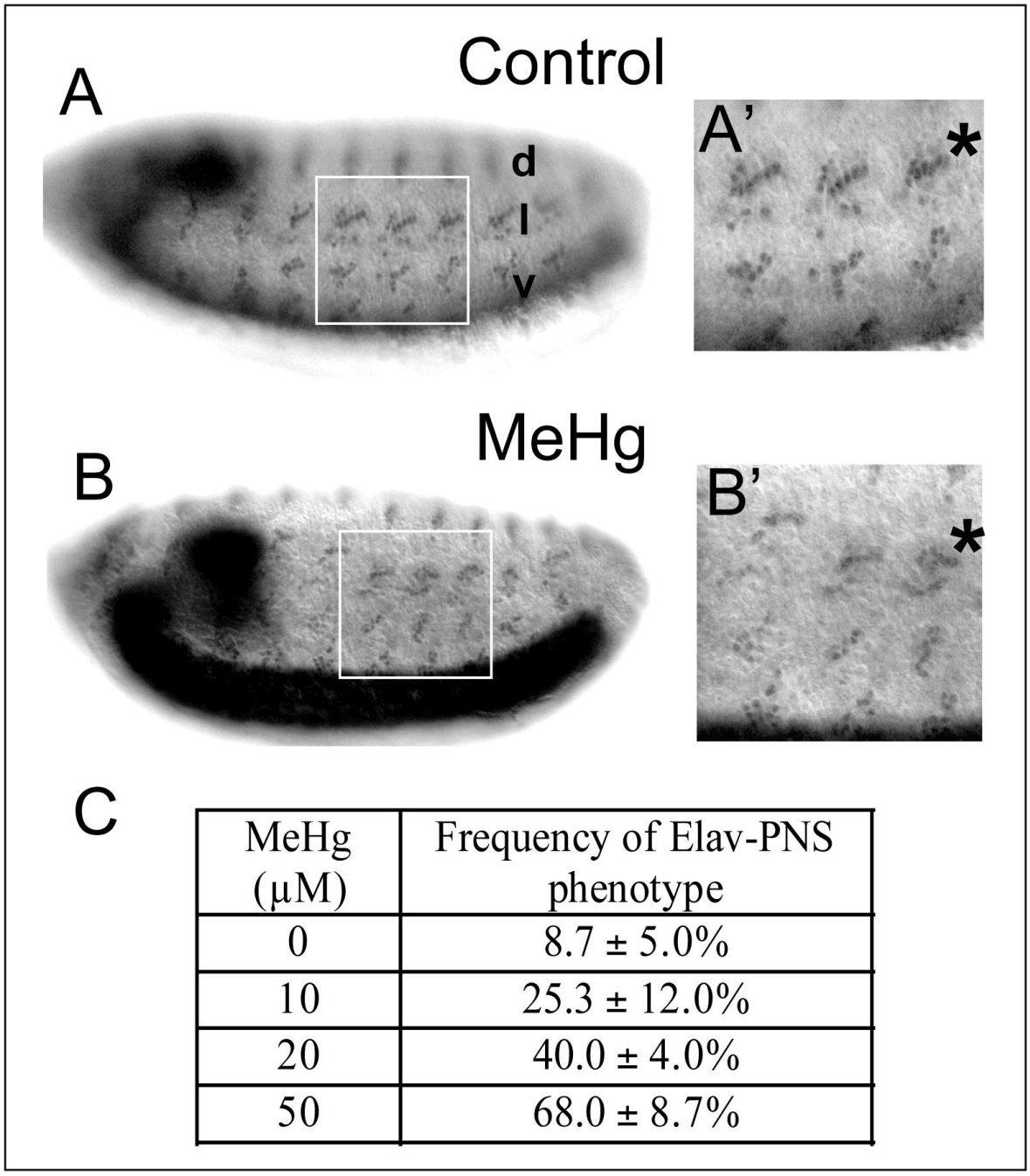

C

MeHg (μM)	Frequency of Elav-PNS phenotype
0	8.7 ± 5.0%
10	25.3 ± 12.0%
20	40.0 ± 4.0%
50	68.0 ± 8.7%

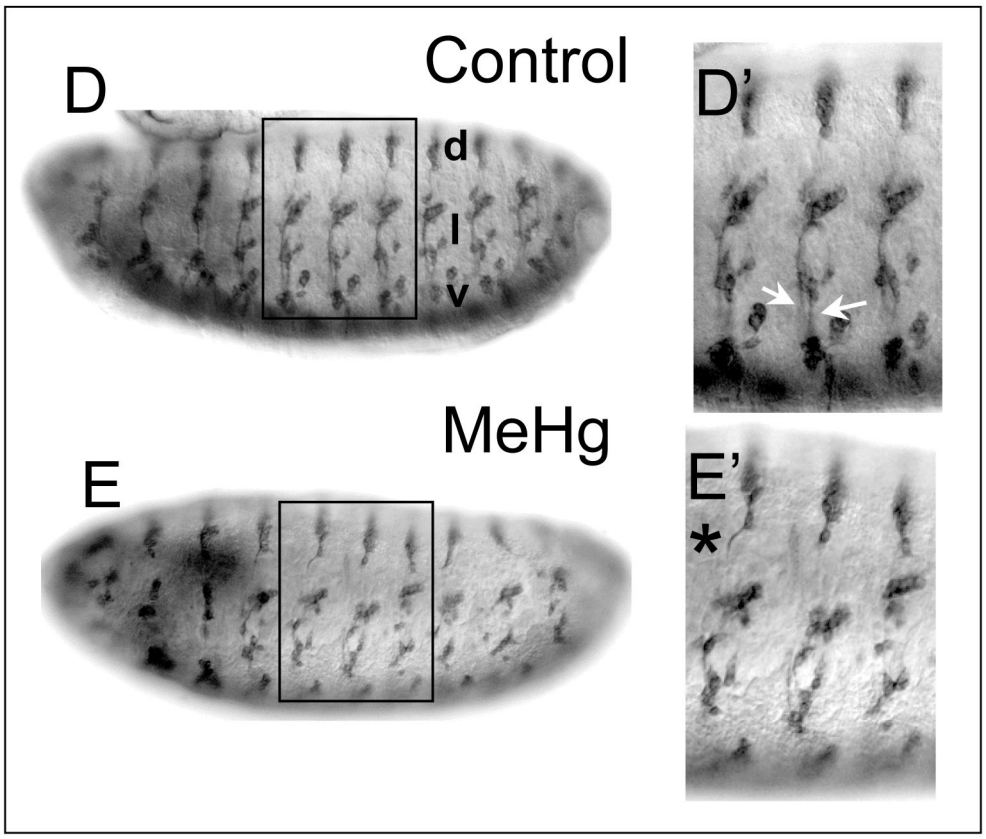

Figure 6. Defects in neural patterning and axon outgrowth in the PNS of MeHg treated embryos

Patterning of stage 14–15 embryos PNS neurons with control (A) and MeHg (50μM) exposure (B) is revealed with the anti-elav antibody. The dorsal (d), lateral (l) and ventral (v) clusters of the PNS sensory neurons form in a stereotypical pattern in each abdominal segment (A, A ′) that is disrupted with MeHg exposure (B, B′). The lateral lch5 neuron cluster is denoted by (*). (Note, the intensity difference of the VNC staining arises from the slightly different orientation of the embryos in A versus B) The frequency of the MeHg-induced PNS phenotype at various MeHg concentrations is seen in the table (C) (see methods). Average and standard deviation of three independent MeHg treatments for each concentration are shown with n=150 embryos for each data point. Axon projections of stage 14–15 embryo PNS neurons with control (D) and MeHg (50μM) treatment (E) are revealed by staining with the 22C10/Futstch antibody. Normal projections of the segmental and intersegmental nerves (white arrows, D′) in control embryos and the abnormal projection of the dorsal nerve (* E′) with MeHg are shown. (Anterior is to the left and dorsal is up. See text for discussion).

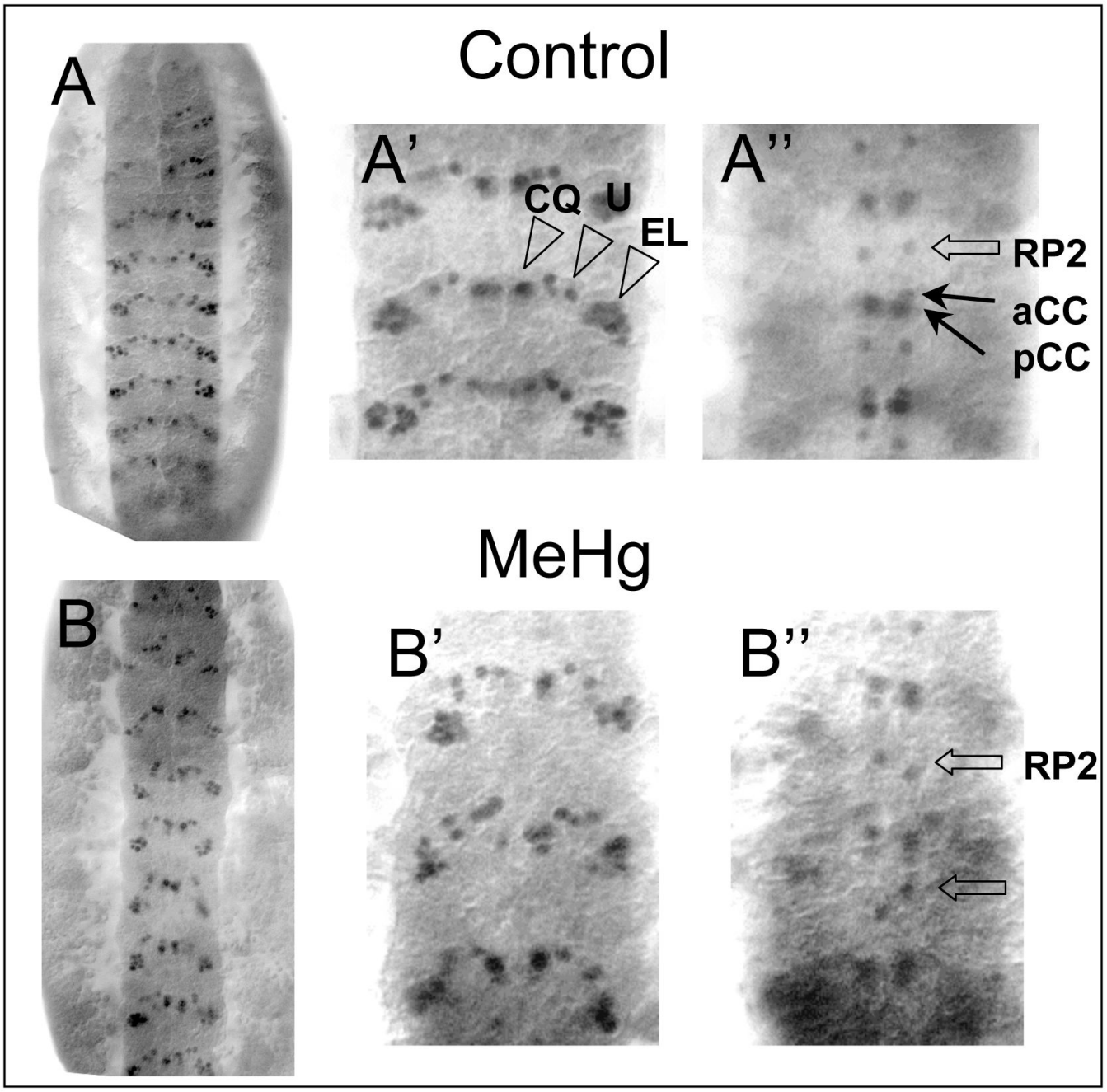

Figure 7. Defects in neural patterning in the CNS of MeHg treated embryos

Patterning of stage 14–15 embryo CNS neurons with control (A) and MeHg (50μM) exposure (B) is revealed with the anti-Even-skipped antibody (a ventral view with the anterior up). The clusters of the CQ, U and EL neurons in the ventral region of the VNC of three abdominal segments is shown in A′ and B′. Orientation of the RP, aCC and pCC neurons in the dorsal region of the VNC are shown in A″ and B″ (See text for discussion).

B

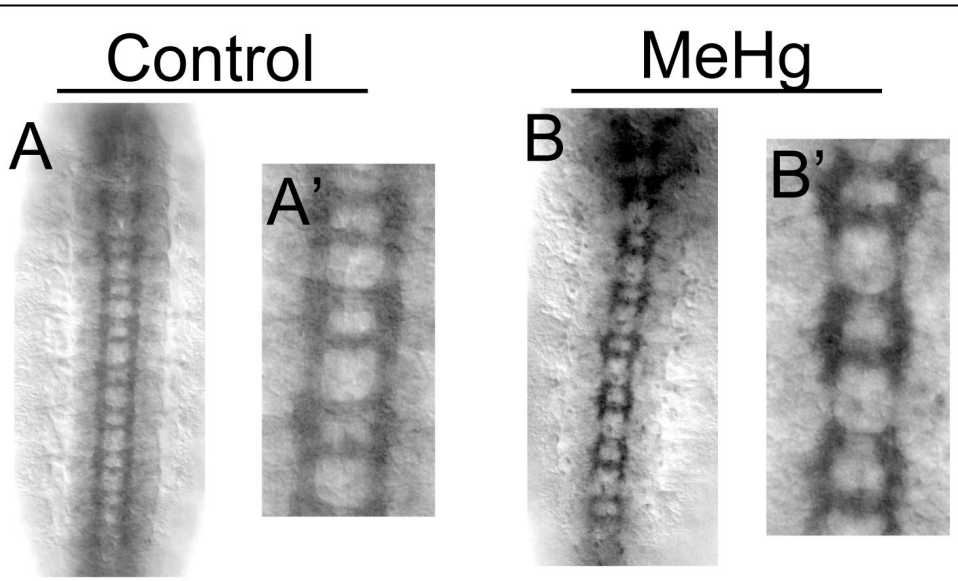

C

MeHg (μM)	Frequency of BP102-CNS phenotype
0	11.1 ± 1.0%
20	35.0 ± 4.8%
50	46.3 ± 4.9%

Figure 8. Defects in CNS axonal projections in MeHg treated embryos

Axon tracts of stage 14–15 embryo CNS neurons with control (A) and MeHg (50μM) treatment (B) are revealed by staining with the BP102 antibody. BP102 labels longitudinal and commissural bundles of CNS neuron axons. MeHg causes a reduction in the formation ans size of longitudinal and commisuarl axon bundles (B, B′). Average and standard deviation of four independent MeHg treatments for each concentration are shown with n<280 embryos for each data point (C) (See text for discussion).

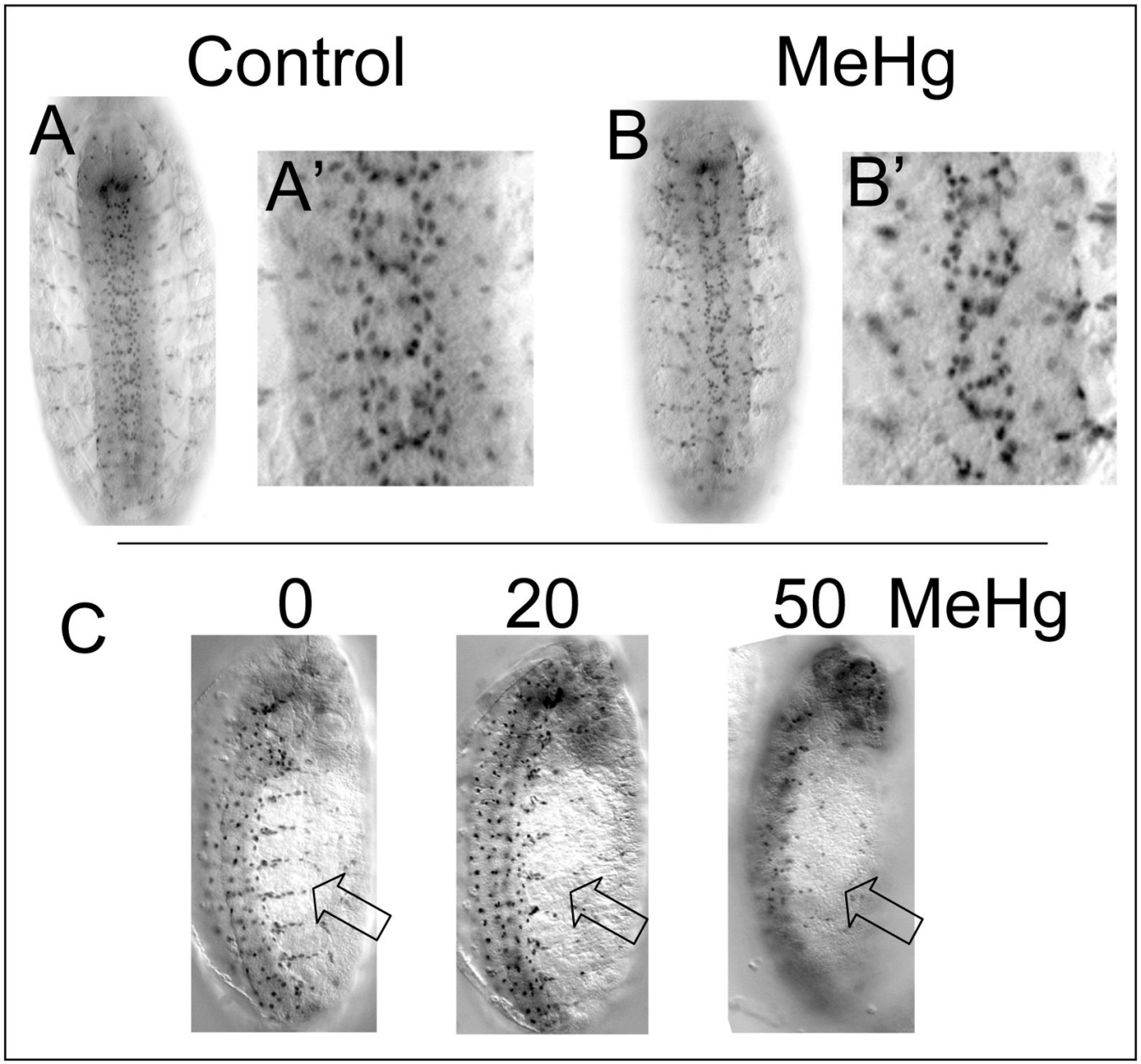

Figure 9. Defects in glial patterning in MeHg treated embryos

CNS and PNS glia of stage 14–15 embryos CNS neurons with control (A) and MeHg (50μM) treatment (B) are revealed by staining with the anti-Repo antibody. Concentration dependent effects on glia in the PNS (open arrow) are seen with MeHg treatment (C) (See text for discussion).

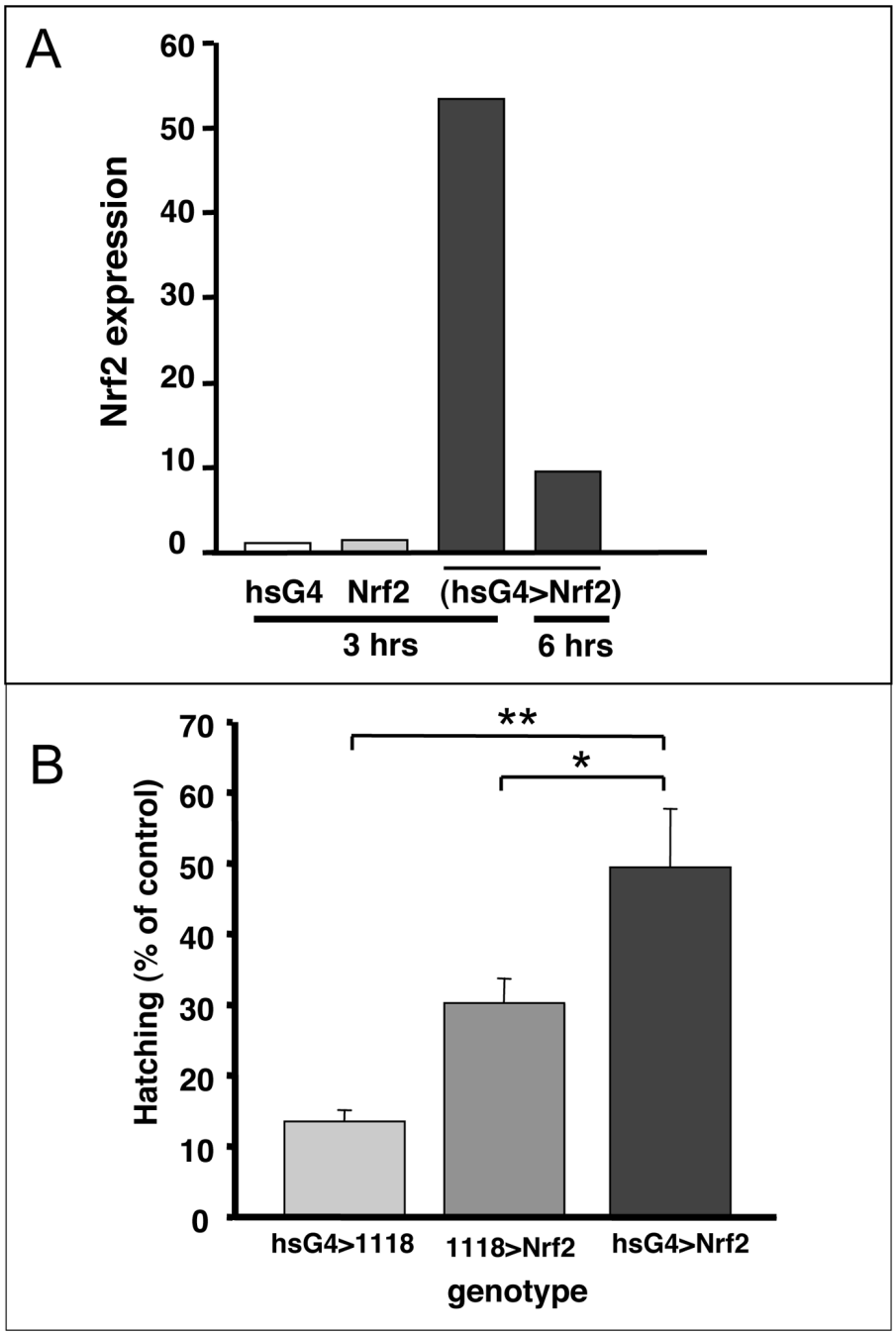

Figure 10. Nrf2 expression confers tolerance to MeHg in embryo hatching

(A) Nrf2 is expressed in transgenic embryos carrying the heatshockGal4>UAS-Nrf2 (hsG4>Nrf2) constructs. Four-hour-old embryos induced by a heat pulse are recovered for the times indicated (see methods). Levels of Nrf2 expression are shown, as determined by qPCR and normalization to expression in the hsG4 parent line. (B) Embryo hatching rate of the hsG4>Nrf2 and control crosses are shown in the presence of 20 MeHg. Percent hatching with MeHg is expressed relative to hatching rate in the absence of MeHg (See methods for details). Values are mean and standard deviation of three experiments with n>400 embryos for each treatment. (* = p=<0.05, ** = p<0.005 using Student's *t* test).